



Article

Antibiofilm Activity of Protamine Against the Vaginal Candidiasis Isolates of *Candida albicans*, *Candida tropicalis* and *Candida krusei*

Sivakumar Jeyarajan ^{1,2,†} , Indira Kandasamy ^{1,†}, Raja Veerapandian ^{3,4} , Jayasudha Jayachandran ¹, Shona Chandrashekar ¹, Kalimuthusamy Natarajaseenivasan ^{3,5}, Prahalathan Chidambaram ⁶ and Anbarasu Kumarasamy ^{1,*}

¹ Microbial Biotechnology Laboratory, Department of Marine Biotechnology, Bharathidasan University, Tiruchirappalli 620024, Tamil Nadu, India; jeyaraja@umich.edu (S.J.); kindirabsc@gmail.com (I.K.)

² Transgenic Animal Model Core, Biomedical Research Core Facilities, University of Michigan, Ann Arbor, MI 48108, USA

³ Department of Microbiology, Bharathidasan University, Tiruchirappalli 620024, Tamil Nadu, India; r.veerapandian@ttuhsc.edu (R.V.); director-rmrcne@icmr.gov.in (K.N.)

⁴ Center of Emphasis in Infectious Diseases, Department of Molecular and Translational Medicine, Paul L. Foster School of Medicine, Texas Tech University Health Sciences Center El Paso, El Paso, TX 79905, USA

⁵ Indian Council of Medical Research, Regional Medical Research Centre, Dibrugarh 786010, Assam, India

⁶ Department of Biochemistry, Bharathidasan University, Tiruchirappalli 620024, Tamil Nadu, India; prahalath@bdu.ac.in

* Correspondence: anbumbt@bdu.ac.in

† These authors contributed equally to this work.

Abstract: *Candida* species, normally part of the healthy human flora, can cause severe opportunistic infections when their population increases. This risk is even greater in immunocompromised individuals. Women using intrauterine contraceptive devices (IUDs) are at higher risk for IUD-associated vulvovaginal candidiasis (VVC) because the device provides a surface for biofilm formation. This biofilm formation allows the normal flora to become opportunistic pathogens, leading to symptoms of VVC such as hemorrhage, pelvic pain, inflammation, itching and discharge. VVC is often linked to IUD use, requiring the prompt removal of these devices for effective treatment. This study evaluated the activity of the arginine-rich peptide “protamine” against *Candida albicans*, *Candida tropicalis* and *Candida krusei* isolated from IUD users who had signs of VVC. The antimicrobial activity was measured using the agar disk diffusion and microbroth dilution methods to determine the minimum inhibitory concentration (MIC). The MIC values of protamine against *C. albicans*, *C. tropicalis* and *C. krusei* are 32 $\mu\text{g mL}^{-1}$, 64 $\mu\text{g mL}^{-1}$ and 256 $\mu\text{g mL}^{-1}$, respectively. The determined MIC of protamine was used for a biofilm inhibition assay by crystal violet staining. Protamine inhibited the biofilm formation of the VVC isolates, and its mechanisms were studied through scanning electron microscopy (SEM) and a reactive oxygen species (ROS) assay. The disruption of cell membranes and the induction of oxidative stress appear to be key mechanisms underlying its anti-candidal effects. The results from an in vitro assay support the potential use of protamine as an antibiofilm agent to coat IUDs in the future for protective purposes.

Keywords: antifungal peptides; protamine; multi-drug resistance; *Candida* spp.; biofilm inhibition; intrauterine contraceptive devices (IUDs); vulvovaginal candidiasis



Academic Editor: Nicolai S. Panikov

Received: 8 December 2024

Revised: 13 January 2025

Accepted: 16 January 2025

Published: 23 January 2025

Citation: Jeyarajan, S.; Kandasamy, I.; Veerapandian, R.; Jayachandran, J.; Chandrashekar, S.; Natarajaseenivasan, K.; Chidambaram, P.; Kumarasamy, A. Antibiofilm Activity of Protamine Against the Vaginal Candidiasis Isolates of *Candida albicans*, *Candida tropicalis* and *Candida krusei*. *Appl. Biosci.* **2025**, *4*, 5. <https://doi.org/10.3390/applbiosci4010005>

Copyright: © 2025 by the authors.

Licensee MDPI, Basel, Switzerland.

This article is an open access article distributed under the terms and conditions of the Creative Commons Attribution (CC BY) license

(<https://creativecommons.org/licenses/by/4.0/>).

1. Introduction

Candidiasis, caused by *Candida* species, has become a significant global health issue in recent years [1,2]. This is largely due to the growing resistance of these infections to existing antifungal medications like fluconazole, echinocandins and polyenes. Vulvovaginal candidiasis (VVC) is a condition in women that causes vaginal discharge, pruritus, pelvic pain and inflammation. Globally, 70–75% of women experience VVC at least once during their reproductive years [1,2]. VVC can be acute or chronic, significantly impacting women's quality of life by causing persistent discomfort and stress and the disruption of daily activities and mental health. The incidence of vaginitis caused by non-albicans *Candida* (NAC) species is increasing, posing significant challenges due to their reduced susceptibility to fluconazole, a commonly used drug. NAC infections are often recurrent.

VVC is frequently diagnosed based on non-specific symptoms and treated without culture confirmation in most developing and less-developed countries. The widespread use of oral fluconazole for prophylaxis, especially in immunocompromised patients such as those with HIV [3] or organ transplant recipients, further contributes to resistance in *Candida* spp. [4]. In particular, NAC species are inherently resistant to azoles, which cause adverse reactions when administered to immunocompromised individuals. This has prompted clinicians to explore alternate treatment strategies.

Intrauterine devices (IUDs) are used worldwide for contraception. However, these devices are sites of attraction for commensal microorganisms like bacteria and *Candida* spp. These commensals adhere to IUDs and form biofilms. This biofilm can lead to a significant increase in their numbers, transforming the commensals into pathogens. IUDs can thus become reservoirs for *Candida* infections, accumulating larger biofilm masses and contributing to recurrent infections [5]. This pathogenicity causes inflammation in the surrounding tissues, leading to disease and a weakened immune system. The outgrowth of *Candida* spp. on these devices exacerbates vaginal candidiasis, causing alarm and a loss of confidence among users. Thus, VVC can become invasive, leading to candidemia. The progression from using a contraceptive device to a life-threatening condition is concerning and often overlooked. Although amphotericin B is a last-resort antifungal treatment, it is generally not prescribed for vaginal candidiasis to avoid resistance development. Unfortunately, resistance to amphotericin B has also been observed [6,7]. In cases of resistance, physicians may increase the dose, which is toxic to patients and causes further complications. The World Health Organization (WHO) reports that immunocompromised IUD users are at higher risk of VVC [8]. The high mortality rate associated with these infections underscores the urgent need for effective infection control measures and anti-*Candida* treatments.

Candida spp. develops resistance by molecular mechanisms that are ultimately responsible for phenotype change in their cells. The molecular mechanisms involve the overexpression or mutation of the target enzyme [9], the alteration of the enzyme in the same biosynthetic pathway as the target enzyme, the upregulation of drug efflux pumps (ATP binding cassette), the upregulation of virulent gene expression, etc. The physical mechanisms include dimorphic transitions, i.e., phenotypic switching from a budding yeast cell to a filamentous form, which helps the pathogen evade the drug and adapt to invade host epithelial tissues [10]. Additionally, pleiotropic changes in target structures render the drug incapable of binding to its target. The transformation into persister cells, which remain in a dormant state, makes the molecular targets of *Candida* spp. inactive [11]. Furthermore, the formation of a matrix prevents anti-*Candida* drugs from reaching their targets. Most pathogenic *Candida* spp. are shielded by this matrix, which facilitates biofilm formation. The biofilm formed on the matrix prevents antimicrobial substances from reaching individual cells. Biofilm-associated cells require concentrations of fluconazole and amphotericin B that are 1000 times higher than those needed for planktonic cells [12,13] to inhibit the

Candida spp.-associated biofilms. These characteristics play a crucial role in the persistent recurrence of infections and antibiotic resistance. These traits pose additional difficulties in orchestrating a successful treatment strategy for *Candida* infections, necessitating new therapeutics that can overcome the above problems.

Recent research has focused on cationic antimicrobial peptides (AMPs), which are toxic to *Candida* spp. but harmless to normal mammalian cells [14,15]. This selectivity is due to differences in the membrane properties and composition of *Candida* spp. and mammalian cells. AMPs are composed of repeating sequences of positively charged and hydrophobic amino acids, giving them amphiphilic properties. These amphiphilic properties allow AMPs to bind to the negatively charged *Candida* spp. membrane components (β -glucan, chitin and phosphomannoproteins) and penetrate the hydrophobic membrane, forming channels that cause cytosolic content leakage. Since AMPs target negative charges rather than specific carbohydrate or lipid moieties, the likelihood of resistance is low. Histatins [16], protonectin [17], LL-37 in humans [18], the N-terminal domain of bovine lactoferrin [19], epinecidin-1 [20–24], synthetic helical peptides [25] and KABT-AMP [11] are a few examples of AMPs that have an anti-*Candida* effect.

Protamine is a small, arginine-rich “MPRRRRSSSRPVRRRRRSRRRRRRGRRRR” (NCBI accession # P69014) nuclear protein that replaces histone late in the haploid phase of spermatogenesis and is essential for sperm head condensation and DNA stabilization. Protamine was discovered in salmon testicles by Fredrich Miescher in 1869 and identified in the folding of nucleic acids in salmon sperm. Protamine has been approved by the FDA for injection or infusion into blood vessels to treat heparin overdose [26]. It is also used as an insulin carrier in the form of isophane insulin and sold by Eli Lilly. Protamine has been used as a gene delivery agent with minimal toxicity [27,28]. Protamine has also been shown to inhibit protease produced by bacteria [29]. Protamine has several characteristics, including high stability under heat and pH, that make it suitable for use as a preservative in neutral or alkaline food [30].

In this study, we experimentally determined the susceptibility of VVC isolates to protamine by the microbroth dilution method to determine the minimum inhibitory concentration (MIC). To study the mechanism of action, crystal violet staining, scanning electron microscopy (SEM) and a reactive oxygen species (ROS) assay were used. The experimental observations revealed that protamine has a MIC of 32 $\mu\text{g mL}^{-1}$ against *C. albicans*, 64 $\mu\text{g mL}^{-1}$ against *C. tropicalis* and 256 $\mu\text{g mL}^{-1}$ against *C. krusei*. The microscopic analysis revealed that protamine disrupts the *Candida* spp. membrane and generates reactive oxygen species for lysing the *Candida* spp. cells.

2. Materials and Methods

2.1. *Candida* Isolates and Strains

The vulvovaginal candidiasis (VVC) isolates *C. tropicalis* (strain CA4) and *C. krusei* (strain CA54), with high biofilm-forming potential, which were reported by Shanmugapriya et al. [31], were used to evaluate the anti-*Candida* efficacy of protamine. The above two strains were isolated from women, aged 20–35 years, who had signs of pelvic inflammation, hemorrhage and vaginal discharge at the gynecological and obstetrics unit of Pankajam Seetharaman Hospital, Tiruchirapalli, Tamil Nadu, India, reported by Shanmugapriya et al. [31]. Endocervical swabs from the removed IUD devices were taken from each patient, grown on CHROM agar and identified for non-albicans *Candida* (NAC). Twenty-three clinical NAC isolates (10 of *C. krusei* and 13 of *C. tropicalis*) were the most pervasive non-albicans *Candida* (NAC). Among them, *C. tropicalis* (strain CA4) and *C. krusei* (strain CA54) were found to be resistant to amphotericin B, with high biofilm-forming potential containing several microcolonies. A pathogenic strain of *C. albicans* resistant to fluconazole [32] was

obtained from the Microbial Type Culture Collection (cat. no. MTCC 227) and used as a control test organism.

2.2. Protamine and Chemicals

Protamine (cat. no. 3369), Sabouraud Dextrose Broth (SDB; cat. no. 108339), Whatman No.1 sterile disks (cat. no. WHA2017006), 2',7'-dichlorofluorescein diacetate (DCFH-DA; cat. no. D6883), Hoechst (cat. no. 63493) and glutaraldehyde (cat. no. G5882) were from Sigma Aldrich (Millipore Sigma Burlington, MA, USA). All additional chemical reagents employed in the testing procedures were of analytical grade and obtained from Hi-media (Hi-media Ltd., Mumbai, India).

2.3. Assessment of the Anti-Candidal Activity of Protamine Using Disk Diffusion

The anti-candidal activity of protamine was evaluated by the agar disk diffusion method. Briefly, one hundred microliters of *Candida* spp. (10^6 cells) were spread uniformly across the Sabouraud dextrose agar (SDA) culture plates individually. Protamine was dissolved in phosphate-buffered saline (PBS, pH 7.4) to 1 mg mL^{-1} . Whatman paper disks impregnated with protamine at concentrations of 10 μg , 20 μg , 30 μg , 40 μg and 50 μg were placed on the surface of the agar and incubated at 37°C for 24 h so that the peptide diffused from the filter paper into the agar. Post 24 h, the zone of inhibition (ZOI) was measured and plotted as the mean of three experimental measurements.

2.4. Anti-Candidal Assay for Minimum Inhibitory Concentration (MIC) Determination

The antimicrobial activity of protamine against *C. tropicalis* (strain CA4), *C. krusei* (strain CA54) and *C. albicans* (MTCC 227) was tested with the growth media: Sabouraud Dextrose Broth (SDB). The microbroth dilution method was used in accordance with the Clinical and Laboratory Standards Institute (CLSI) M27-Ed4 guidelines for anti-*Candida* susceptibility testing [33]. The stock solution of protamine was diluted with phosphate-buffered saline (PBS) to reach concentrations of 1, 2, 4, 8, 16, 32, 64, 128, 256 and 512 $\mu\text{g mL}^{-1}$ [11]. Aliquots (20 μL) from each dilution were distributed in a 96-well polystyrene microtiter plate, and each well was inoculated with a 180 μL suspension of *Candida* spp. in SDB containing 1×10^6 cells. Cultures were grown with gentle shaking for 24 h at 37°C . Wells containing only the *Candida* spp. cells without a peptide were used as growth or positive controls, and plain broth was used as a sterility or negative control. The absorbance was evaluated at 595 nm using a microplate reader (Bio-Rad, Hercules, CA, USA) and represented in terms of the percentage of growth using a growth control value of 100% growth. The minimal inhibitory concentration (MIC) of protamine was defined as the lowest concentration at which a percentage of growth of less than 15% was observed. The antimicrobial assay was performed in triplicate, and the growth percentage was plotted as mean \pm S.D.

2.5. Biofilm Assay

To determine the ability of protamine to inhibit biofilm formation, a 1 mL suspension of *Candida* spp. (1×10^6 cells) in SDB media was seeded into each well of a 24-well plate containing microscope coverslip (circular borosilicate cover glasses (15 mm), Fisher Scientific, Hampton, NH, USA) inserts [11]. The cover glass served as a substratum for microbial attachment. Protamine at its MIC concentration against *Candida* spp. was treated for 24 h, using 32 $\mu\text{g mL}^{-1}$ of *C. albicans*, 64 $\mu\text{g mL}^{-1}$ of *C. tropicalis* and 256 $\mu\text{g mL}^{-1}$ of *C. krusei*. After incubation, the spent media was aspirated, and 1 mL of 0.1% (*w/v*) crystal violet dissolved in PBS was added to each well and incubated for 30 min to stain the cells. Post staining, excess crystal violet was removed by washing twice with PBS. The cells were fixed with 4%

formaldehyde (*v/v*), washed with PBS and dehydrated with 80% (*v/v*) ethanol. The stained coverslips were examined under a light microscope with 40× magnification.

2.6. Scanning Electron Microscopy (SEM)

To view the morphological changes in the *C. albicans* cells (MTCC 227) after treatment with protamine, SEM was employed [34]. In brief, *C. albicans* cells were grown to a logarithmic phase with an inoculum size of 1×10^6 cells on a microscope coverslip, which was inserted into each well of a 24-well dish. Protamine at its MIC concentration of $32 \mu\text{g mL}^{-1}$ against *C. albicans* was added to the culture medium. *C. albicans* grown without any peptide was used as a negative control. After 6 h of incubation at 37 °C, the cells were washed twice with phosphate-buffered saline (PBS) pH 7.4 and metabolically fixed with an equal volume of 5% (*v/v*) glutaraldehyde at 4 °C overnight. The metabolically fixed cells were dehydrated with a serial gradient of ethanol wash from 70 to 100%. The coverslips were then sputter-coated and examined under a scanning electron microscope (VEGA3 TESCAN, Czech Republic).

2.7. Measurement of Cellular ROS Production

The ROS generated after treatment with protamine were measured by a fluorometric assay with 2',7'-dichlorofluorescein diacetate (DCFHDA), as described in [17]. Briefly, *Candida* spp. (1×10^6 cells) were seeded into 24-well polystyrene plates and treated with or without protamine at their respective MIC for each species for 24 h. After 24 h of treatment, the cells were incubated with 10 μM of DCFH-DA for 1 h and washed with PBS pH 7.4. They were then visualized under a fluorescent microscope (Accu-Scope, EXI-310, Commack, NY, USA) at 10× magnification and documented with green channel fluorescence intensities (excitation of 488 nm and emission of 525 nm, respectively). Hoechst dye ($5 \mu\text{g mL}^{-1}$ final concentration) was added along with DCFH-DA in PBS to stain the nucleus. Blue channel fluorescence intensities (excitation of 355 nm and emission of 465 nm) were used for imaging the Hoechst stain.

3. Results

3.1. Susceptibility of VVC *Candida* spp. Isolates to Protamine

The susceptibility of the VVC *Candida* spp. isolates to the antimicrobial peptide protamine was determined by the agar disk diffusion method, also called the zone of inhibition test or Kirby–Bauer method. It is a semi-quantitative method to determine the ability of the peptide to inhibit *Candida* spp. growth. Protamine is added to the disk, and it diffuses through the agar to exert its function. If the peptide is effective against the *Candida* spp., no growth will be observed around the disk. This is the zone of inhibition (ZOI). The ZOI evaluated for protamine against *Candida* spp. is shown in Figure 1a–c, and the measurements are shown in Figure 1d–f. As seen in Figure 1a,b, *C. albicans* and *C. tropicalis* are sensitive to protamine; however, *C. krusei* is not sensitive to protamine at the concentrations tested (10 to 50 μg). A maximum ZOI of 1.5 cm was observed for *C. albicans*; it was 1.5 cm at 40 and 50 μg of protamine. For *C. tropicalis*, a gradient increase in the ZOI was observed from 20 to 50 μg of protamine. However, for *C. krusei*, no ZOI was observed from 10 to 50 μg of protamine, which led us to determine the minimum inhibitory concentration (MIC) of protamine by the broth dilution method that can be used for anti-*Candida* activity.

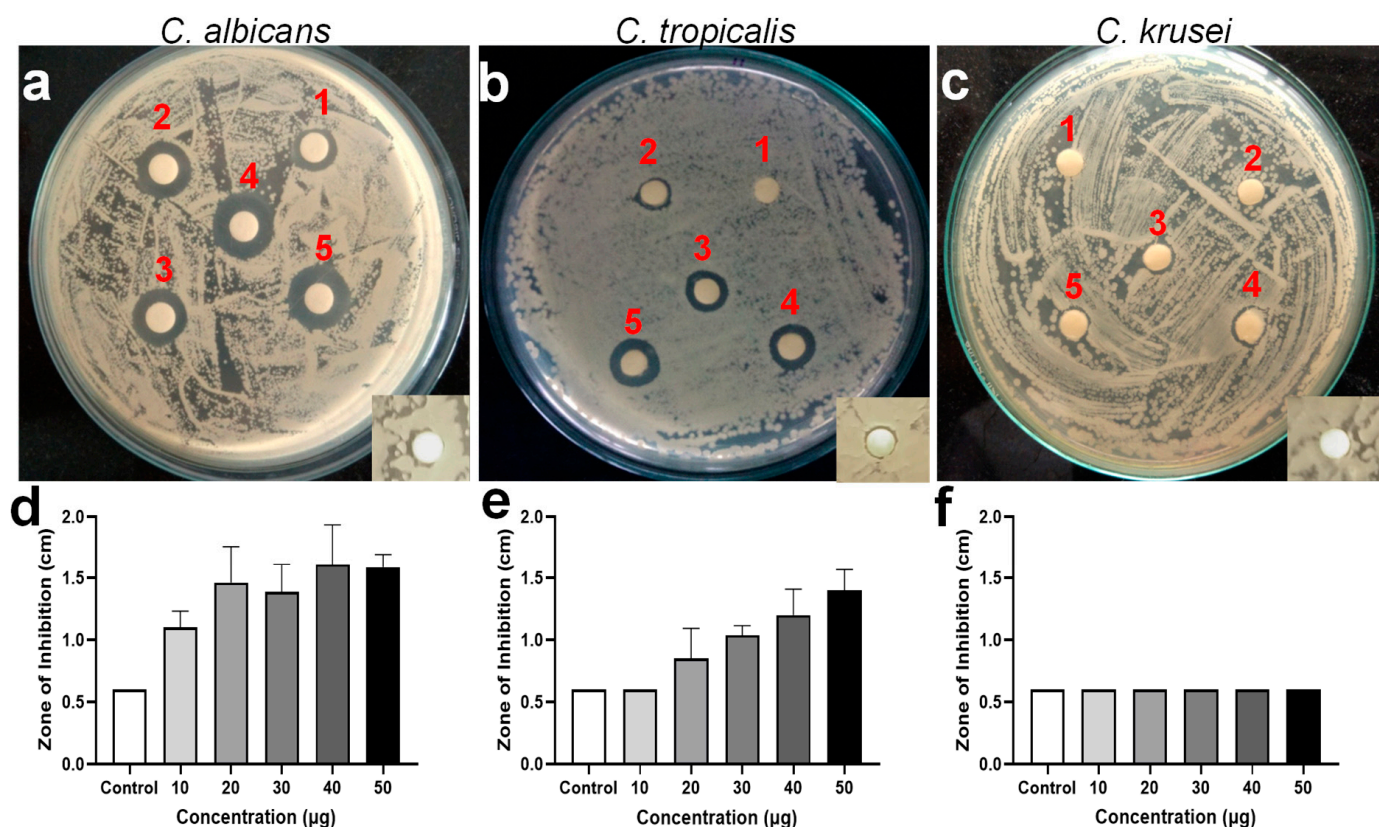


Figure 1. Susceptibility of (a) *C. albicans* (MTCC 227), VVC *Candida* spp. isolates, (b) *C. tropicalis* (CA4) and (c) *C. krusei* (CA54) to protamine measured by an agar diffusion assay. The numbers marked on the plate images refer to the concentration of protamine loaded onto the disks (1–10, 2–20, 3–30, 4–40 and 5–50 µg). The inset shows the image of a disk loaded with PBS as a control. The bar graphs (d–f) below each image show the diameter of the zone of inhibition (ZOI) plotted for each concentration for each species. The control shows the diameter of the disk alone (0.6 cm). For *C. albicans* and *C. krusei*, a concentration gradient increase in the ZOI was observed. For *C. krusei*, no ZOI was observed for the measured concentrations of 10 to 50 µg.

3.2. Protamine Inhibits the Growth of VVC *Candida* spp. Isolates

The *Candida*-cidal activity of protamine against the VVC isolates was studied using the microbroth dilution method to quantitatively determine their growth, as measured by the optical density at 595 nm. Figure 2 shows the plot of the growth of the isolates treated with protamine at a range of concentrations (1 to 512 µg mL⁻¹). The percentage of growth was measured by normalizing them against the cells grown without peptides, which were considered 100%. The minimum inhibitory concentration (MIC) for protamine against the VVC isolates was determined from the lowest concentration at which the growth was inhibited. Protamine inhibited the growth of *C. albicans* at 32 µg mL⁻¹, that of *C. tropicalis* at 64 µg mL⁻¹ and that of *C. krusei* at 256 µg mL⁻¹. At this concentration, the wells inoculated with protamine showed no turbidity.

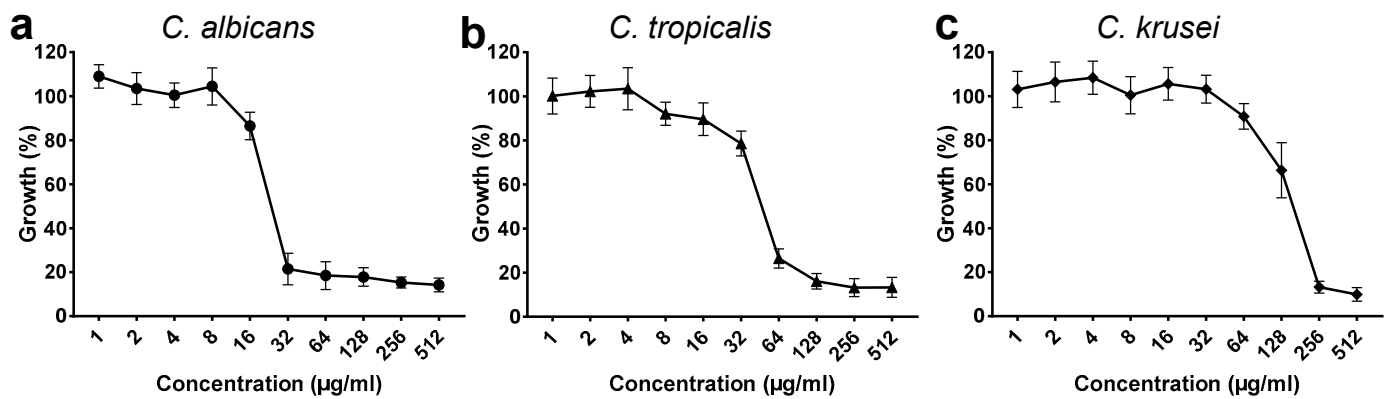


Figure 2. *Candida*-cidal activity of protamine against *Candida* spp. (a–c). A microbroth dilution assay was performed from 0 to 512 $\mu\text{g mL}^{-1}$ to determine the MIC. Cell densities for *Candida* spp. measured at 595 nm without protamine are used as controls with 100% growth. The MIC of protamine is 32 $\mu\text{g mL}^{-1}$ against *C. albicans*, 64 $\mu\text{g mL}^{-1}$ against *C. tropicalis* and 256 $\mu\text{g mL}^{-1}$ against *C. krusei*.

3.3. Protamine Inhibits the Biofilm Formation of VVC Isolates

After determining the MIC, the ability of protamine to prevent the biofilm formation of VVC isolates formed on glass coverslips was determined by crystal violet staining. As these isolates were reported to form biofilm [31], they were cultured with and without protamine at its MIC against the VVC isolates for 24 h. After the treatment period, the coverslips containing the *Candida* spp. cells were stained with crystal violet and then examined under an inverted 40 \times light microscope (Figure 3). The images shown in Figure 3d–f provide visible evidence of protamine’s ability to inhibit biofilm formation. The control samples (*Candida* spp. cells without peptides) showed dense cell clusters indicative of a substantial biofilm. The protamine-treated cover glass did not have a dense biofilm matrix and showed a significant reduction in cell numbers

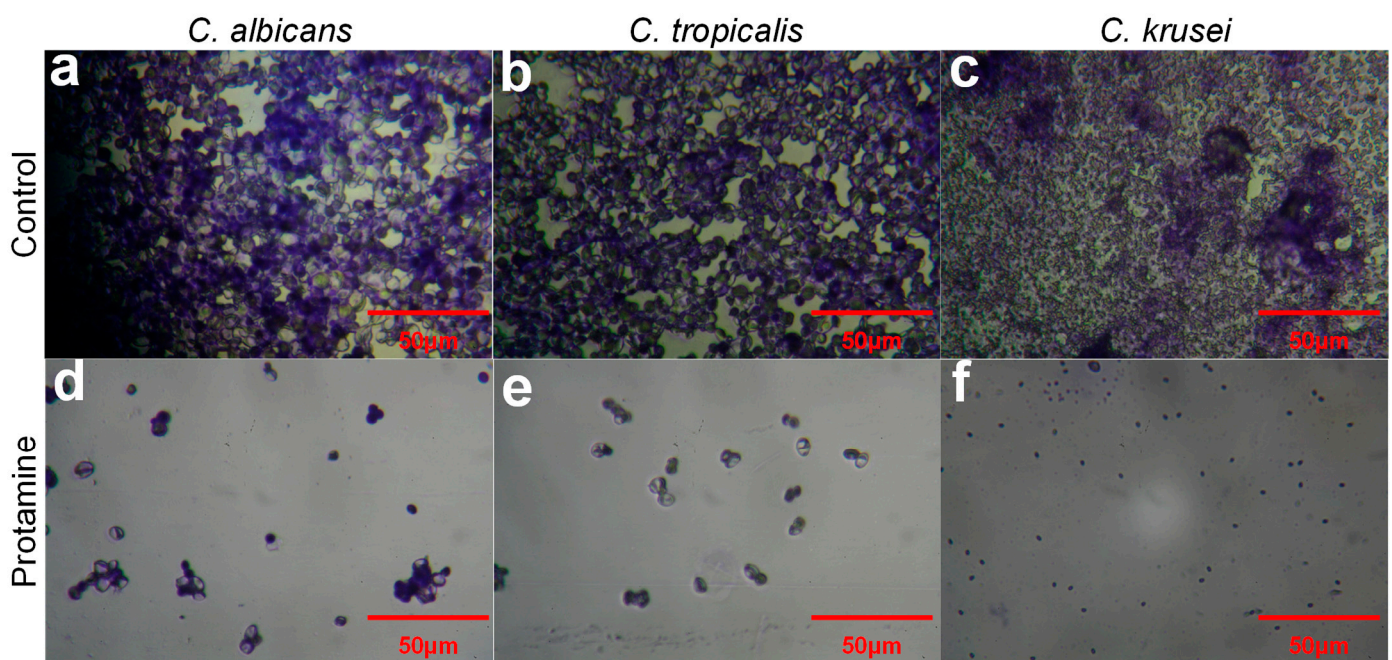


Figure 3. Light microscopic image of crystal violet-stained control cells: (a) *C. albicans*, (b) *C. tropicalis* (CA4) and (c) *C. Krusei* (CA54) at 40 \times magnification. The cells (d–f) were treated with 32, 64 and 256 $\mu\text{g mL}^{-1}$ of protamine, respectively, for 24 h and stained with crystal violet.

3.4. Protamine Disrupts *C. albicans* Membrane Integrity

Scanning electron microscopy (SEM) was utilized to investigate the impact of protamine on cell wall disruption efficiency in the *C. albicans* cells, as illustrated in Figure 4. In the SEM field, the untreated control *C. albicans* cells are seen stacked on one another as a thick layer of biofilm and exhibit typical features: an oval shape, a smooth surface, polar buds and bud scars. The protamine-treated *C. albicans* cells ($32 \mu\text{g mL}^{-1}$ for 6 h) are fewer in number, with empty space in the field and between the cells. The protamine-treated cells in the field appear shrunk, imploded and plasmolyzed. Some cells exhibit surface deformations, including rough textures, disruption, structural destabilization and cell wall collapse.

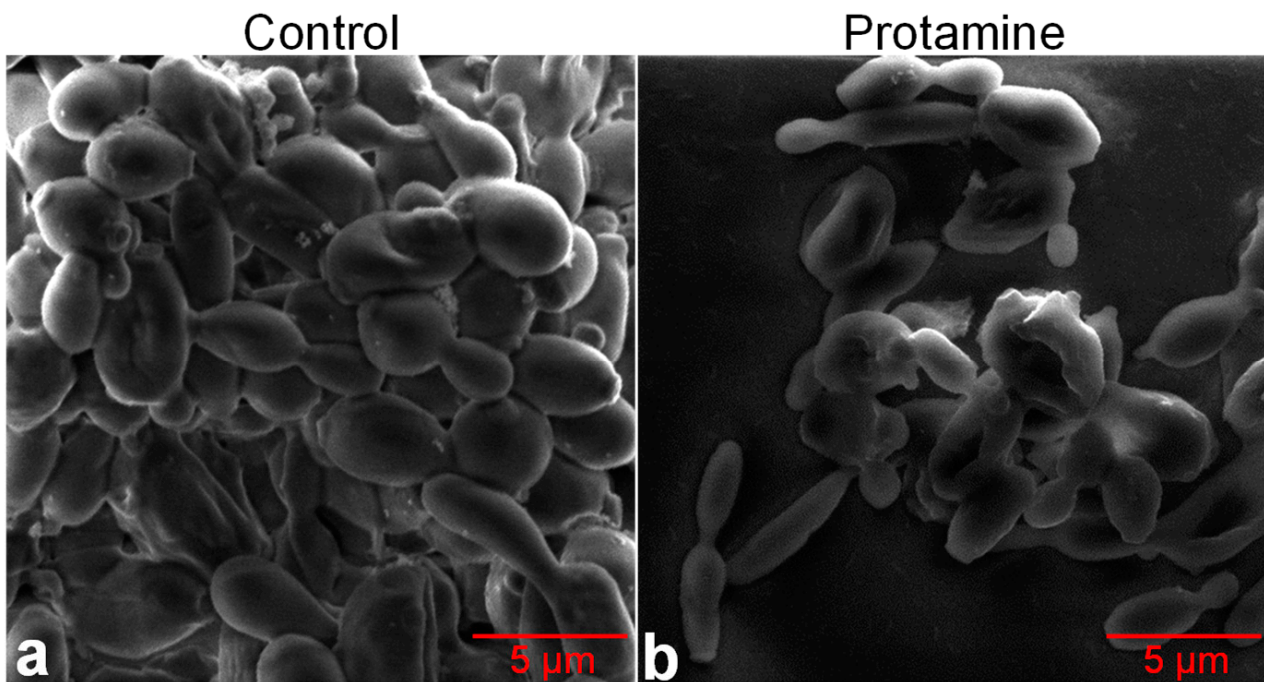


Figure 4. Scanning electron microscopic (SEM) image of *C. albicans* (MTCC 227): (a) the control and (b) protamine-treated cells. *C. albicans* was treated with protamine at $32 \mu\text{g mL}^{-1}$ for 6 h. A reduction in the number of cells is noted as well as empty spaces between the cells and the disruption of the cell wall, demonstrating the lytic activity of protamine. The protamine-treated cells show plasmolysis and a ruptured surface, with internally collapsed morphology due to cytoplasm leakage and a shrunk appearance with grooves compared to the control cells.

3.5. Protamine Treatment Induces ROS Generation

The present study evaluated whether the membrane perturbation generated ROS because of more complex intracellular signaling events, like the oxidation of phospholipids and other macromolecules. Protamine's ability to induce ROS formation was analyzed by using the cell-permeant fluorogenic dye DCFDA. DCFDA is a cell-permeant dye that is oxidized to yield fluorescence when exposed to ROS. The fluorescence can be monitored with an excitation wavelength of 488 nm and an emission wavelength of 525 nm. As illustrated in Figure 5, no bright-green fluorescence is observed in the control *Candida* spp. The phase image shows a dense cell population. Protamine treatment showed a phased reduced cell density and induced ROS production, inferred by the presence of bright-green-colored cells in the field compared to the background green fluorescence observed in the control.

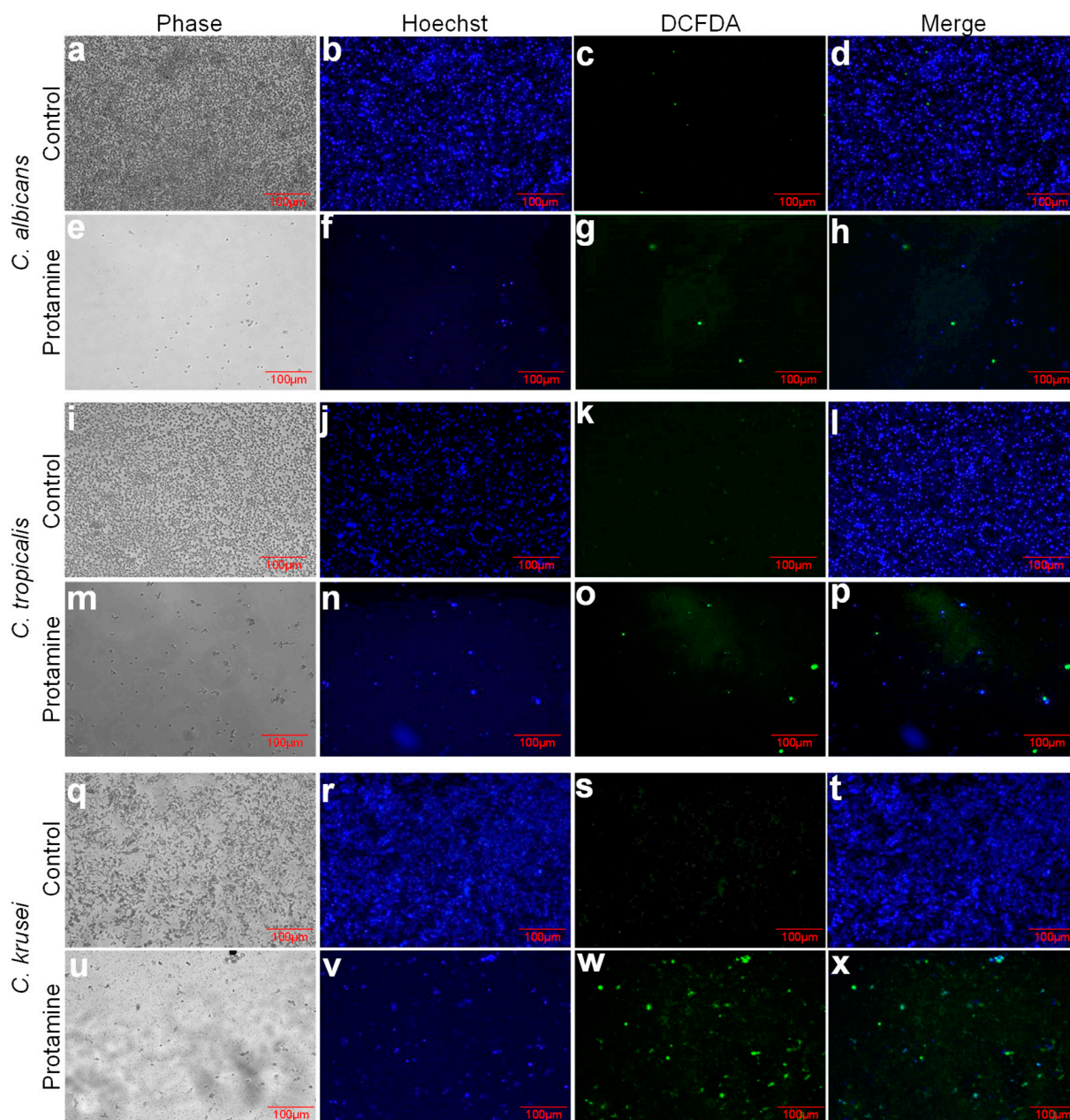


Figure 5. Effect of protamine on ROS production in *Candida* spp. Protamine at its MIC was added to VVC *Candida* spp. isolates, and ROS generation was studied using DCFH-DA. The nonfluorescent dye DCFH-DA at a concentration of 10 μ M was pre-incubated with *Candida* spp. and allowed to grow for 24 h at 37 °C with and without protamine. After 24 h, the culture dish was washed with PBS (pH 7.4) and observed under a fluorescent microscope. The images were captured at an excitation wavelength of 488 nm and an emission wavelength of 525 nm for the DCFH-DA. The generation of ROS will result in DCFH-DA fluorescence. Although the control cells did not exhibit any fluorescence, the cells treated with protamine at their MIC displayed green fluorescence. Hoechst dye was used to stain the nucleus and appears blue. For protamine-treated cells, there is less blue fluorescence (both in the number of cells and intensity), showing signs of a damaged nucleus. The top two rows of panels show *C. albicans* without (a–d) and with (e–h) protamine. The two middle rows of panels represent *C. tropicalis* treated with (m–p) and without (i–l) protamine. *C. krusei* with (u–x) and without (q–t) protamine is shown in the bottom two rows of panels.

4. Discussion

According to the Center for Disease Control (CDC), candidemia accounts for 25% of mortality among patients hospitalized due to implanted device-related bloodstream

infections [35,36]. *C. albicans* is the most prominent species causing candidiasis; however, in recent years, occurrences of non-*albicans Candida* (NAC) have been increasing. The general prescription of azoles to treat candidiasis is the cause of the NAC increase because NAC is inherently resistant to fluconazole, a commonly prescribed drug for candidiasis. This is the primary reason for evaluating the susceptibility of VVC isolates, *C. tropicalis* and *C. krusei* to protamine in this study.

Antimicrobial peptides (AMPs) are short cationic amphiphilic peptides, which exhibit helical or beta-sheet structures that facilitate the peptide to penetrate microbial cells specifically because of their anionic membrane (β -glucan, chitin and phosphomannoproteins) [37,38]. Short AMPs also form aggregates that cause cell death [11,25,39–43], as defined by the carpet model mechanism of action [44]. AMPs have been studied pre-clinically and clinically to treat candidiasis. Human lactoferrin-derived peptide hLF1-11 was studied in clinical trials for its anti-candidemia effect [45,46]. The synthetic AMP PL-18 is under clinical trial for treating vaginal colpomycosis, bacterial vaginosis and mixed vaginitis. PL-18 was loaded into suppositories for this purpose [47]. CZEN-002, a synthetic octapeptide derived from the α -melanocyte stimulating hormone (α -MSH), was studied for treating vulvovaginal candidiasis as a topical application.

Fascinated by the potential of AMPs to specifically kill pathogens, we evaluated the antibiofilm potential of an arginine-rich AMP named protamine. Protamine has been reported to have antimicrobial activity against periodontopathic bacteria such as *Porphyromonas gingivalis*, *Prevotella intermedia* and *Aggregatibacter actinomycetemcomitans* [48]. Protamine has also been reported to show antimicrobial activity against catheter-associated *E. coli*, *Klebsiella pneumoniae*, *Pseudomonas aeruginosa*, *Staphylococcus epidermidis* and *Enterococcus faecalis* biofilms in combination with ciprofloxacin [49] or chlorhexidine [50]. It also acts as an N-acetyl-D-glucosamine-1-phosphate acetyltransferase (GlmU) inhibitor to inhibit cell wall biosynthesis in Gram-negative and Gram-positive bacteria [51]. Additionally, it has been shown to possess anti-candidal activity against *Candida albicans* isolated from poly(methyl methacrylate) (PMMA) dental prostheses [52].

Given that protamine has been reported to exhibit antimicrobial activity against microbes associated with urinary catheters and dental prostheses, we investigated its anti-*Candida* and antibiofilm properties against non-*albicans Candida* isolates linked to IUD-associated vulvovaginal candidiasis (VVC). Initially we used the agar disk diffusion method to determine susceptibility and found that *C. albicans* and *C. tropicalis* were sensitive to protamine, with a maximum zone of inhibition (ZOI) of 1.5 cm observed for *C. albicans* at concentrations of 40 and 50 μg , while *C. tropicalis* exhibited a gradient increase in ZOI from 0.8 to 1.1 cm for concentrations of 20 to 50 μg . In contrast, *C. krusei* showed no susceptibility to protamine at the tested concentrations (10 to 50 μg). Because more protamine could not be added to the disk, we used the microbroth dilution method to measure the minimum inhibitory concentration (MIC) of protamine against the VVC isolates. By the microbroth dilution method, the lowest concentrations required to inhibit the growth of *C. albicans*, *C. tropicalis* and *C. krusei* are 32 $\mu\text{g mL}^{-1}$, 64 $\mu\text{g mL}^{-1}$ and 256 $\mu\text{g mL}^{-1}$, respectively, which are their MIC. In summary, while the agar disk diffusion method offers a visual and semi-quantitative assessment of susceptibility, the broth dilution method provides definitive MIC values that are crucial for understanding the effective concentrations needed for antimicrobial action. Both methods together reinforce the conclusion that protamine has significant anti-candidal activity.

After determining the MIC, the ability of protamine to inhibit the biofilm formation of vulvovaginal candidiasis (VVC) isolates on glass coverslips was investigated at their MIC. The results of the study demonstrate that protamine effectively inhibits biofilm formation on glass coverslips by vulvovaginal candidiasis (VVC) isolates, as evidenced by crystal

violet staining. The control samples, which did not receive protamine treatment, exhibited dense cell clusters indicative of substantial biofilm formation. In contrast, the cells on the coverslips treated with protamine showed a significant reduction in cell numbers and lacked the dense biofilm matrix, highlighting protamine's ability to inhibit biofilm development. The images captured under a 40× light microscope provide clear visual evidence of this inhibitory effect, with treated samples displaying fewer cells and less structural integrity compared to the controls.

SEM analysis performed to explore how protamine affects the cell wall integrity of *C. albicans* revealed that protamine induces structural deformities and disrupts its organization and plasmolysis, primarily through electrostatic interactions. Strong, positively charged protamine binds with negatively charged phosphomannoproteins in the *Candida* spp. cell wall. This binding causes cell wall damage, as observed in the field, such as doughnut-shaped shrunken cells, which is a sign of the efflux of cytoplasmic components from the cells, possibly due to the formation of pores. These observations align with previously documented mechanisms, such as the dilation of ionic channels by protamine sulfate, which aids in transporting antibiotics into the cytoplasm [53], and the leakage of potassium ions, ATP and intracellular enzymes from the cells due to the increase in membrane permeability [54–57]. Additionally, protamine has been shown to enhance membrane-ATPase activity, further contributing to membrane permeability [58].

AMPs can generate various reactive oxygen species (ROS), such as superoxide anions ($O_2^{\bullet-}$), hydroxyl radicals (OH^{\bullet}), hydroperoxyl (HO_2^{\bullet}), singlet oxygen (1O_2) [59] and hydrogen peroxide (H_2O_2) [60], as part of their pathogen-killing mechanism. We evaluated the ROS generation ability of protamine in pathogenic *Candida* spp. using DCFH-DA. DCFH-DA is a widely used dye for assaying oxidative activity in live cells. As a nonfluorescent lipophilic probe, it can cross the cell membrane. Inside the cell, DCFH-DA is deacetylated to form DCFH₂, which is also nonfluorescent and unable to diffuse freely across the cell membrane. DCFH₂ reacts with intracellular ROS, mainly through peroxy products (H_2O_2) and peroxy radicals (ROO^{\bullet}) [61], to produce the fluorescent DCF. Although the oxidation of DCFH₂ is not directly sensitive to singlet oxygen, singlet oxygen can indirectly contribute to DCF formation through its reaction with the cellular substrates that yield (H_2O_2) [61]. Given the evidence that short aggregating peptides produce hydrogen peroxide (H_2O_2), DCFH-DA is indeed the most suitable dye for detecting ROS generated by protamine. This dye effectively measures oxidative activity in live cells by reacting with intracellular ROS to produce a fluorescent signal, making it ideal for such studies. The obtained results for increased ROS by protamine treatment are comparable to those from previous studies on antimicrobials and antimicrobial peptides (AMPs), such as polymyxin B [62–64], plant defensins [65], colistin [66], lactoferricin B [67] and protonectin B [17].

In this study, we found evidence that protamine increases the levels of peroxy products (H_2O_2) and peroxy radicals (ROO^{\bullet}). To determine if protamine also increases superoxide levels, dyes such as singlet oxygen sensor green (SOSG) can be used in combination with superoxide inhibitors like N-acetylcysteine (NAC). Additionally, HKOH-1 [68] can be used for the specific detection of hydroxyl radicals. Furthermore, assessing oxidative damage to macromolecules such as proteins, lipids and DNA, which are targets of protamine, can be achieved by measuring protein carbonyls, malondialdehyde and 8-Hydroxy-2'-deoxyguanosine (8-OHdG). This approach will help us understand the detailed mechanism of protamine action.

Since protamine is clinically used to counteract heparins preoperatively or during cardiac surgery, it also has potential applications as an anti-candidal agent to disrupt biofilm on IUDs. The median lethal dose (LD50) of protamine sulfate reported for rabbits and mice was found to be between 200 mg/kg and 300 mg/kg when given subcutaneously [50]. This

provides evidence that coating IUDs with protamine will be highly beneficial to inhibiting biofilm formation and does not cause harm to the host.

5. Conclusions

In this study, we experimentally confirmed that protamine can disrupt the membrane of *Candida* spp. using antimicrobial susceptibility, biochemical and morphological assays. The mechanism of cell death involves protamine binding, which alters the transmembrane potential and disrupts cation flux. This binding to the membrane also causes structural stress and deformities, allowing external oxygen to penetrate the cells and oxidize phospholipids and macromolecules, thereby disrupting their function. The continued presence of protamine leads to cell membrane damage and cytoplasmic efflux. These findings provide proof of concept for designing protamine-coated intrauterine devices (IUDs) and medical implants where biofilm formation is a significant concern.

Author Contributions: Conceptualization: S.J., I.K., R.V., J.J., S.C., K.N., P.C. and A.K.; methodology: S.J., J.J., S.C. and A.K.; software: S.J., J.J., S.C. and A.K.; validation: S.J. and A.K.; formal analysis: S.J., J.J., S.C. and A.K.; investigation: A.K.; resources: S.J., A.K., K.N. and P.C.; data curation: S.J., J.J., S.C. and A.K.; writing—original draft preparation: S.J., J.J., S.C. and A.K.; writing—review and editing: S.J., J.J., S.C. and A.K.; visualization: S.J. and A.K.; supervision, A.K.; project administration, A.K., P.C. and K.N.; funding acquisition, S.J., A.K., P.C. and K.N. All authors have read and agreed to the published version of the manuscript.

Funding: This research was funded by the Department of Biotechnology, India (Ref. No. BT/PR2071/BBE/117/241/2016), RUSA 2.0 Biological Sciences (Ref. No. 311/RUSA(2.0)/2018), Bharathidasan University, Tiruchirappalli, and Tamil Nadu State Council for Higher Education (TANSCHÉ) (Ref. No. 01706/P6/2021).

Institutional Review Board Statement: Not applicable.

Informed Consent Statement: Not applicable.

Data Availability Statement: Data are contained within the article.

Acknowledgments: S.J. acknowledges the Indian Council of Medical Research (ICMR-NET-61754/2010) for granting fellowship. We thank National College, Tiruchirappalli, India, for performing the scanning electron microscopy studies.

Conflicts of Interest: The authors declare no conflicts of interest.

Abbreviations

ABC	ATP binding cassette
AMP	Antimicrobial peptide
CDC	Center for Disease Control
DCFHDA	2',7'-dichlorofluorescein diacetate
MIC	Minimum inhibitory concentration
PBS	Phosphate-buffered saline
ROS	Reactive oxygen species
VVC	Vulvovaginal candidiasis

References

1. Sobel, J.D. Recurrent vulvovaginal candidiasis. *Am. J. Obs. Gynecol.* **2016**, *214*, 15–21. [[CrossRef](#)]
2. Mariyah, S.; Iyer, R.N.; Jangam, R.R.; Kesireddy, S. Vulvovaginal candidiasis: Clinical profile, species distribution and antifungal susceptibility pattern. *J. Acad. Clin. Microbiol.* **2022**, *24*, 71–75.

3. Guideline Development Group; Saxon, C.; Edwards, A.; Rautemaa-Richardson, R.; Owen, C.; Nathan, B.; Palmer, B.; Wood, C.; Ahmed, H.; Ahmad, S.; et al. British Association for Sexual Health and HIV national guideline for the management of vulvovaginal candidiasis (2019). *Int. J. STD AIDS* **2020**, *31*, 1124–1144. [[CrossRef](#)] [[PubMed](#)]
4. Jothi, R.; Sangavi, R.; Raja, V.; Kumar, P.; Pandian, S.K.; Gowrishankar, S. Alteration of Cell Membrane Permeability by Cetyltrimethylammonium Chloride Induces Cell Death in Clinically Important Candida Species. *Int. J. Environ. Res. Public Health* **2022**, *20*, 27. [[CrossRef](#)]
5. Auler, M.E.; Morreira, D.; Rodrigues, F.F.; Abr Ao, M.S.; Margarido, P.F.; Matsumoto, F.E.; Silva, E.G.; Silva, B.C.; Schneider, R.P.; Paula, C.R. Biofilm formation on intrauterine devices in patients with recurrent vulvovaginal candidiasis. *Med. Mycol.* **2010**, *48*, 211–216. [[CrossRef](#)]
6. Ahmady, L.; Gothwal, M.; Mukkoli, M.M.; Bari, V.K. Antifungal drug resistance in Candida: A special emphasis on amphotericin B. *Apmis* **2024**, *132*, 291–316. [[CrossRef](#)]
7. Carolus, H.; Sofras, D.; Boccarella, G.; Sephton-Clark, P.; Biriukov, V.; Cauldron, N.C.; Lobo Romero, C.; Vergauwen, R.; Yazdani, S.; Pierson, S.; et al. Acquired amphotericin B resistance leads to fitness trade-offs that can be mitigated by compensatory evolution in *Candida auris*. *Nat. Microbiol.* **2024**, *9*, 3304–3320. [[CrossRef](#)]
8. World Health Organization. *Recommendations for the Treatment of Trichomonas Vaginalis, Mycoplasma Genitalium, Candida Albicans, Bacterial Vaginosis and Human Papillomavirus (Anogenital Warts): Web Annex C: Evidence-to-Decision Framework and Systematic Review for the WHO Treatment Recommendations for Candida Albicans*; World Health Organization: Geneva, Switzerland, 2024.
9. Lee, Y.; Robbins, N.; Cowen, L.E. Molecular mechanisms governing antifungal drug resistance. *NPJ Antimicrob. Resist.* **2023**, *1*, 5. [[CrossRef](#)]
10. Calderone, R.A.; Fonzi, W.A. Virulence factors of *Candida albicans*. *Trends Microbiol.* **2001**, *9*, 327–335. [[CrossRef](#)]
11. Thankappan, B.; Jeyarajan, S.; Hiroaki, S.; Anbarasu, K.; Natarajaseenivasan, K.; Fujii, N. Antimicrobial and antibiofilm activity of designed and synthesized antimicrobial peptide, KABT-AMP. *Appl. Biochem. Biotechnol.* **2013**, *170*, 1184–1193. [[CrossRef](#)]
12. Pereira, R.; dos Santos Fontenelle, R.O.; de Brito, E.H.S.; de Morais, S.M. Biofilm of *Candida albicans*: Formation, regulation and resistance. *J. Appl. Microbiol.* **2021**, *131*, 11–22. [[CrossRef](#)] [[PubMed](#)]
13. Chandra, J.; Mukherjee, P.K. Candida Biofilms: Development, Architecture, and Resistance. *Microbiol. Spectr.* **2015**, *3*, 115–134. [[CrossRef](#)] [[PubMed](#)]
14. Freitas, C.G.; Felipe, M.S. *Candida albicans* and Antifungal Peptides. *Infect. Dis. Ther.* **2023**, *12*, 2631–2648. [[CrossRef](#)]
15. Perez-Rodriguez, A.; Eraso, E.; Quindós, G.; Mateo, E. Antimicrobial Peptides with Anti-Candida Activity. *Int. J. Mol. Sci.* **2022**, *23*, 9264. [[CrossRef](#)]
16. Jang, W.S.; Li, X.S.; Sun, J.N.; Edgerton, M. The P-113 fragment of histatin 5 requires a specific peptide sequence for intracellular translocation in *Candida albicans*, which is independent of cell wall binding. *Antimicrob. Agents Chemother.* **2008**, *52*, 497–504. [[CrossRef](#)] [[PubMed](#)]
17. Wang, K.; Dang, W.; Xie, J.; Zhu, R.; Sun, M.; Jia, F.; Zhao, Y.; An, X.; Qiu, S.; Li, X.; et al. Antimicrobial peptide protonectin disturbs the membrane integrity and induces ROS production in yeast cells. *Biochim. Biophys. Acta* **2015**, *1848 Pt A*, 2365–2373. [[CrossRef](#)]
18. Ordonez, S.R.; Amarullah, I.H.; Wubbolts, R.W.; Veldhuizen, E.J.A.; Haagsman, H.P. Fungicidal mechanisms of cathelicidins LL-37 and CATH-2 revealed by live-cell imaging. *Antimicrob. Agents Chemother.* **2014**, *58*, 2240–2248. [[CrossRef](#)] [[PubMed](#)]
19. Mishra, B.; Leishangthem, G.D.; Gill, K.; Singh, A.K.; Das, S.; Singh, K.; Xess, I.; Dinda, A.; Kapil, A.; Patro, I.K.; et al. A novel antimicrobial peptide derived from modified N-terminal domain of bovine lactoferrin: Design, synthesis, activity against multidrug-resistant bacteria and *Candida*. *Biochim. Biophys. Acta* **2013**, *1828*, 677–686. [[CrossRef](#)]
20. Jeyarajan, S.; Peter, A.S.; Sathyan, A.; Ranjith, S.; Kandasamy, I.; Duraisamy, S.; Chidambaram, P.; Kumarasamy, A. Expression and purification of epinecidin-1 variant (Ac-Var-1) by acid cleavage. *Appl. Microbiol. Biotechnol.* **2024**, *108*, 176. [[CrossRef](#)] [[PubMed](#)]
21. Jeyarajan, S.; Sathyan, A.; Peter, A.S.; Ranjith, S.; Duraisamy, S.; Natarajaseenivasan, S.M.; Chidambaram, P.; Kumarasamy, A. Bioproduction and Characterization of Epinecidin-1 and Its Variants Against Multi Drug Resistant Bacteria Through In Silico and In Vitro Studies. *Int. J. Pept. Res. Ther.* **2023**, *29*, 66. [[CrossRef](#)]
22. Jeyarajan, S.; Peter, A.S.; Ranjith, S.; Sathyan, A.; Duraisamy, S.; Kandasamy, I.; Chidambaram, P.; Kumarasamy, A. Glycine-replaced epinecidin-1 variant bestows better stability and stronger antimicrobial activity against a range of nosocomial pathogenic bacteria. *Biotechnol. Appl. Biochem.* **2024**, *71*, 1384–1404. [[CrossRef](#)] [[PubMed](#)]
23. Jeyarajan, S.; Kumarasamy, A. Anti-Candida and antibiofilm activity of epinecidin-1 and its variants. *bioRxiv* **2024**. [[CrossRef](#)]
24. Jeyarajan, S.; Ranjith, S.; Veerapandian, R.; Natarajaseenivasan, K.; Chidambaram, P.; Kumarasamy, A. Antibiofilm Activity of Epinecidin-1 and Its Variants Against Drug-Resistant *Candida krusei* and *Candida tropicalis* Isolates from Vaginal Candidiasis Patients. *Infect. Dis. Rep.* **2024**, *16*, 1214–1229. [[CrossRef](#)]
25. Thankappan, B.; Sivakumar, J.; Asokan, S.; Ramasamy, M.; Pillai, M.M.; Selvakumar, R.; Angayarkanni, J. Dual antimicrobial and anticancer activity of a novel synthetic α -helical antimicrobial peptide. *Eur. J. Pharm. Sci.* **2021**, *161*, 105784. [[CrossRef](#)] [[PubMed](#)]

26. Taneja, R.; Szoke, D.J.; Hynes, Z.; Jones, P.M. Minimum protamine dose required to neutralize heparin in cardiac surgery: A single-centre, prospective, observational cohort study. *Can. J. Anesth./J. Can. D'anesthésie* **2023**, *70*, 219–227. [[CrossRef](#)]
27. Govindarajan, S.; Sivakumar, J.; Garimidi, P.; Rangaraj, N.; Kumar, J.M.; Rao, N.M.; Gopal, V. Targeting human epidermal growth factor receptor 2 by a cell-penetrating peptide–affibody bioconjugate. *Biomaterials* **2012**, *33*, 2570–2582. [[CrossRef](#)] [[PubMed](#)]
28. Jeyarajan, S.; Xavier, J.; Rao, N.M.; Gopal, V. Plasmid DNA delivery into MDA-MB-453 cells mediated by recombinant Her-NLS fusion protein. *Int. J. Nanomed.* **2010**, *5*, 725–733. [[CrossRef](#)]
29. Kontani, M.; Amano, A.; Nakamura, T.; Nakagawa, I.; Kawabata, S.; Hamada, S. Inhibitory effects of protamines on proteolytic and adhesive activities of *Porphyromonas gingivalis*. *Infect. Immun.* **1999**, *67*, 4917–4920. [[CrossRef](#)] [[PubMed](#)]
30. Potter, R.; Truelstrup Hansen, L.; Gill, T.A. Inhibition of foodborne bacteria by native and modified protamine: Importance of electrostatic interactions. *Int. J. Food Microbiol.* **2005**, *103*, 23–34. [[CrossRef](#)] [[PubMed](#)]
31. Shanmughapriya, S.; Sornakumari, H.; Lency, A.; Kavitha, S.; Natarajaseenivasan, K. Synergistic effect of amphotericin B and tyrosol on biofilm formed by *Candida krusei* and *Candida tropicalis* from intrauterine device users. *Med. Mycol.* **2014**, *52*, 853–861. [[CrossRef](#)] [[PubMed](#)]
32. Agarwal, V.; Lal, P.; Pruthi, V. Prevention of *Candida albicans* biofilm by plant oils. *Mycopathologia* **2008**, *165*, 13–19. [[CrossRef](#)] [[PubMed](#)]
33. *CLSI M27 Ed4*; Reference Method for Broth Dilution Antifungal Susceptibility Testing of Yeasts. 4th ed. CLSI Standard M27; Clinical and Laboratory Standards Institute (CLSI): Wayne, PA, USA, 2017.
34. Fischer, E.R.; Hansen, B.T.; Nair, V.; Hoyt, F.H.; Dorward, D.W. Scanning electron microscopy. *Curr. Protoc. Microbiol.* **2012**, Unit 2B.2. [[CrossRef](#)]
35. Centre for Disease Control (CDC). *Invasive Candidiasis Statistics—Google Search*; CDC: Atlanta, GA, USA, 2021; Volume 1, pp. 5–9.
36. Veerapandian, R.; Abdul Azees, P.A.; Viswanathan, T.; Amaechi, B.T.; VEDIYAPPAN, G. Editorial: Developing therapeutics for antimicrobial resistant pathogens. *Front. Cell Infect. Microbiol.* **2022**, *12*, 1083501. [[CrossRef](#)]
37. Sonesson, A.; Ringstad, L.; Andersson Nordahl, E.; Malmsten, M.; Mörgelin, M.; Schmidtchen, A. Antifungal activity of C3a and C3a-derived peptides against *Candida*. *Biochim. Biophys. Acta (BBA)-Biomembr.* **2007**, *1768*, 346–353. [[CrossRef](#)] [[PubMed](#)]
38. Harris, M.; Mora-Montes, H.M.; Gow, N.A.R.; Coote, P.J. Loss of mannosylphosphate from *Candida albicans* cell wall proteins results in enhanced resistance to the inhibitory effect of a cationic antimicrobial peptide via reduced peptide binding to the cell surface. *Microbiology* **2009**, *155*, 1058–1070. [[CrossRef](#)] [[PubMed](#)]
39. Anbarasu, K.; Sivakumar, J. Multidimensional significance of crystallin protein–protein interactions and their implications in various human diseases. *Biochim. Biophys. Acta (BBA)-Gen. Subj.* **2016**, *1860*, 222–233. [[CrossRef](#)] [[PubMed](#)]
40. Jeyarajan, S.; Kumarasamy, A.; Cheon, J.; Premceski, A.; Seidel, E.; Kimler, V.A.; Giblin, F.J. TEM analysis of α A66–80 peptide-induced protein aggregates and amyloid fibrils in human and guinea pig α A-crystallins. *Investig. Ophthalmol. Vis. Sci.* **2018**, *59*, 3043.
41. Kumarasamy, A.; Jeyarajan, S.; Kimler, V.A.; Premceski, A.; Cheon, J.; Mishra, V.; Giblin, F.J. In vitro studies on the interaction of guinea pig α A crystallin and α A crystallin (66–80) peptide using fluorescence polarization and transmission electron microscopy. *Investig. Ophthalmol. Vis. Sci.* **2017**, *58*, 5301.
42. Yadav, P.K.; Su, M.; Jeyarajan, S.; Giblin, F.J.; Ohi, M.D. Structural Organization of the Guinea Pig α A-Crystallin and α A66–80 Peptide Complex. *Microsc. Microanal.* **2019**, *25*, 1318–1319. [[CrossRef](#)]
43. Jeyarajan, S.; Kumarasamy, A. Antifungal activity of protamine. *bioRxiv* **2024**. [[CrossRef](#)]
44. Wimley, W.C. Describing the mechanism of antimicrobial peptide action with the interfacial activity model. *ACS Chem. Biol.* **2010**, *5*, 905–917. [[CrossRef](#)] [[PubMed](#)]
45. van der Does, A.M.; Hensbergen, P.J.; Bogaards, S.J.; Cansoy, M.; Deelder, A.M.; van Leeuwen, H.C.; Drijfhout, J.W.; van Dissel, J.T.; Nibbering, P.H. The human lactoferrin-derived peptide hLF1-11 exerts immunomodulatory effects by specific inhibition of myeloperoxidase activity. *J. Immunol.* **2012**, *188*, 5012–5019. [[CrossRef](#)] [[PubMed](#)]
46. van der Does, A.M.; Joosten, S.A.; Vroomans, E.; Bogaards, S.J.; van Meijgaarden, K.E.; Ottenhoff, T.H.; van Dissel, J.T.; Nibbering, P.H. The antimicrobial peptide hLF1-11 drives monocyte-dendritic cell differentiation toward dendritic cells that promote antifungal responses and enhance Th17 polarization. *J. Innate Immun.* **2012**, *4*, 284–292. [[CrossRef](#)]
47. Mercer, D.K.; O'Neil, D.A. Innate inspiration: Antifungal peptides and other immunotherapeutics from the host immune response. *Front. Immunol.* **2020**, *11*, 2177. [[CrossRef](#)] [[PubMed](#)]
48. Miura, T.; Iohara, K.; Kato, T.; Ishihara, K.; Yoshinari, M. Basic peptide protamine exerts antimicrobial activity against periodontopathic bacteria. *J. Biomed. Sci. Eng.* **2010**, *3*, 1069–1072. [[CrossRef](#)]
49. Soboh, F.; Khoury, A.E.; Zamboni, A.C.; Davidson, D.; Mittelman, M.W. Effects of ciprofloxacin and protamine sulfate combinations against catheter-associated *Pseudomonas aeruginosa* biofilms. *Antimicrob. Agents Chemother.* **1995**, *39*, 1281–1286. [[CrossRef](#)] [[PubMed](#)]
50. Darouiche, R.O.; Mansouri, M.D.; Gawande, P.V.; Madhyastha, S. Efficacy of combination of chlorhexidine and protamine sulphate against device-associated pathogens. *J. Antimicrob. Chemother.* **2008**, *61*, 651–657. [[CrossRef](#)] [[PubMed](#)]

51. Suman, E.; D'Souza, S.J.; Jacob, P.; Sushruth, M.R.; Kotian, M.S. Anti-biofilm and anti-adherence activity of Glm-U inhibitors. *Indian J. Med. Sci.* **2011**, *65*, 387–392. [[CrossRef](#)]
52. Miura, T.; Hayakawa, T.; Okumori, N.; Iohara, K.; Yoshinari, M. Antifungal activity against *Candida albicans* on PMMA coated with protamine derivatives. *J. Oral. Tissue Eng.* **2010**, *8*, 30–38. [[CrossRef](#)]
53. Antohi, S.; Popescu, A. Protamine and Polyarginine Bacteriolysis. Similarities in Its Mechanism with Chromatin DNA Picnosis. *Z. Für Naturforschung C* **1979**, *34*, 1144–1150. [[CrossRef](#)]
54. Johansen, C.; Verheul, A.; Gram, L.; Gill, T.; Abee, T. Protamine-induced permeabilization of cell envelopes of gram-positive and gram-negative bacteria. *Appl. Environ. Microbiol.* **1997**, *63*, 1155–1159. [[CrossRef](#)] [[PubMed](#)]
55. Nanda, S.S.; Yi, D.K.; Kim, K. Study of antibacterial mechanism of graphene oxide using Raman spectroscopy. *Sci. Rep.* **2016**, *6*, 28443. [[CrossRef](#)]
56. Jeyarajan, S.; Zhang, I.X.; Arvan, P.; Lentz, S.I.; Satin, L.S. Simultaneous Measurement of Changes in Mitochondrial and Endoplasmic Reticulum Free Calcium in Pancreatic Beta Cells. *Biosensors* **2023**, *13*, 382. [[CrossRef](#)] [[PubMed](#)]
57. Zhang, I.X.; Herrmann, A.; Leon, J.; Jeyarajan, S.; Arunagiri, A.; Arvan, P.; Gilon, P.; Satin, L.S. ER stress increases expression of intracellular calcium channel RyR1 to modify Ca²⁺ homeostasis in pancreatic beta cells. *J. Biol. Chem.* **2023**, *299*, 105065. [[CrossRef](#)] [[PubMed](#)]
58. Aspedon, A.; Groisman, E.A. The antibacterial action of protamine: Evidence for disruption of cytoplasmic membrane energization in *Salmonella typhimurium*. *Microbiology* **1996**, *142 Pt 12*, 3389–3397. [[CrossRef](#)] [[PubMed](#)]
59. Vaishampayan, A.; Grohmann, E. Antimicrobials Functioning through ROS-Mediated Mechanisms: Current Insights. *Microorganisms* **2021**, *10*, 61. [[CrossRef](#)]
60. Raju, M.; Santhoshkumar, P.; Sharma, K.K. Lens Endogenous Peptide α A66-80 Generates Hydrogen Peroxide and Induces Cell Apoptosis. *Aging Dis.* **2017**, *8*, 57–70. [[CrossRef](#)] [[PubMed](#)]
61. Bilski, P.; Belanger, A.G.; Chignell, C.F. Photosensitized oxidation of 2',7'-dichlorofluorescein: Singlet oxygen does not contribute to the formation of fluorescent oxidation product 2',7'-dichlorofluorescein. *Free Radic. Biol. Med.* **2002**, *33*, 938–946. [[CrossRef](#)]
62. Sampson, T.R.; Liu, X.; Schroeder, M.R.; Kraft, C.S.; Burd, E.M.; Weiss, D.S. Rapid killing of *Acinetobacter baumannii* by polymyxins is mediated by a hydroxyl radical death pathway. *Antimicrob. Agents Chemother.* **2012**, *56*, 5642–5649. [[CrossRef](#)] [[PubMed](#)]
63. Velkov, T.; Deris, Z.Z.; Huang, J.X.; Azad, M.A.; Butler, M.; Sivanesan, S.; Kaminskas, L.M.; Dong, Y.D.; Boyd, B.; Baker, M.A.; et al. Surface changes and polymyxin interactions with a resistant strain of *Klebsiella pneumoniae*. *Innate Immun.* **2014**, *20*, 350–363. [[CrossRef](#)]
64. Halder, S.; Yadav, K.K.; Sarkar, R.; Mukherjee, S.; Saha, P.; Haldar, S.; Karmakar, S.; Sen, T. Alteration of Zeta potential and membrane permeability in bacteria: A study with cationic agents. *Springerplus* **2015**, *4*, 672. [[CrossRef](#)] [[PubMed](#)]
65. Cho, Y.; Turner, J.S.; Dinh, N.N.; Lehrer, R.I.; Aerts, A.M.; Bammens, L.; Govaert, G.; Carmona-Gutierrez, D.; Madeo, F.; Cammue, B.P.A.; et al. The Antifungal Plant Defensin HsAFP1 from *Heuchera sanguinea* Induces Apoptosis in *Candida albicans*. *Front. Microbiol.* **2011**, *7*, 47. [[CrossRef](#)]
66. Soon, R.L.; Nation, R.L.; Cockram, S.; Moffatt, J.H.; Harper, M.; Adler, B.; Boyce, J.D.; Larson, I.; Li, J. Different surface charge of colistin-susceptible and -resistant *Acinetobacter baumannii* cells measured with zeta potential as a function of growth phase and colistin treatment. *J. Antimicrob. Chemother.* **2011**, *66*, 126–133. [[CrossRef](#)]
67. Lee, B.; Hwang, J.S.; Lee, D.G. Antibacterial action of lactoferricin B like peptide against *Escherichia coli*: Reactive oxygen species-induced apoptosis-like death. *J. Appl. Microbiol.* **2020**, *129*, 287–295. [[CrossRef](#)]
68. Bai, X.; Huang, Y.; Lu, M.; Yang, D. HKOH-1: A Highly Sensitive and Selective Fluorescent Probe for Detecting Endogenous Hydroxyl Radicals in Living Cells. *Angew. Chem. Int. Ed. Engl.* **2017**, *56*, 12873–12877. [[CrossRef](#)] [[PubMed](#)]

Disclaimer/Publisher's Note: The statements, opinions and data contained in all publications are solely those of the individual author(s) and contributor(s) and not of MDPI and/or the editor(s). MDPI and/or the editor(s) disclaim responsibility for any injury to people or property resulting from any ideas, methods, instructions or products referred to in the content.